Molecular Biology and Evolution

wingless and *aristaless2* Define a Developmental Ground Plan for Moth and Butterfly Wing Pattern Evolution

Arnaud Martin* and Robert D. Reed

Department of Ecology and Evolutionary Biology, University of California, Irvine

***Corresponding author:** E-mail: arnaudm@uci.edu.

Associate editor: Patricia Beldade

Abstract

Butterfly wing patterns have long been a favorite system for studying the evolutionary radiation of complex morphologies. One of the key characteristics of the system is that wing patterns are based on a highly conserved ground plan of pattern homologies. In fact, the evolution of lepidopteran wing patterns is proposed to have occurred through the repeated gain, loss, and modification of only a handful of serially repeated elements. In this study, we examine the evolution and development of stripe wing pattern elements. We show that expression of the developmental morphogen *wingless* (*wg*) is associated with early determination of the major basal (B), discal (DI and DII), and marginal (EI) stripe patterns in a broad sampling of Lepidoptera, suggesting homology of these pattern elements across moths and butterflies. We describe for the first time a novel Lepidoptera-specific homeobox gene, *aristaless2* (*al2*), which precedes *wg* expression during the early determination of DII stripe patterns. We show that *al2* was derived from a tandem duplication of the *aristaless* gene, whereupon it underwent a rapid coding and *cis*-regulatory divergence relative to its more conserved paralog *aristaless1* (*al1*), which retained an ancestral expression pattern. The *al2* stripe expression domain evolutionarily preceded the appearance of the DII pattern elements in multiple lineages, leading us to speculate that *al2* represented preexisting positional information that may have facilitated DII evolution via a developmental drive mechanism. In contrast to butterfly eyespot patterns, which are often cited as a key example of developmental co-option of preexisting developmental genes, this study provides an example where the origin of a major color pattern element is associated with the evolution of a novel lepidopteran homeobox gene.

Key words: evo-devo, wing pattern evolution, lepidoptera, neofunctionalization, developmental drive.

Introduction

There is unity behind the enormous diversity of butterfly and moth wing patterns. Representing one of the most striking examples of morphological variation in the animal kingdom, lepidopteran wing patterns provide a nearly unlimited array of forms that we can use to help us understand how ontogenetic properties can promote trait diversification. Butterfly wings are an example of mosaic evolution, where morphospace can be explored by moderate changes in size, shape, position, and color composition of individual pattern elements (Nijhout 1991). Emerging from this highly modular organization are several implications for our understanding the interaction between morphological evolution and development. First, wing pattern diversity can be viewed as a set of variations on a common theme, resulting from combinations of discrete elements evolving semi-independently (Nijhout 1991). Second, each pattern element has some degree of autonomous developmental control relative to the others (developmental modularity), implying that wings are highly compartmentalized (Carroll et al. 2004; Schlosser and Wagner 2004). Third, the developmental autonomy of each pattern element allows an uncoupling of the variation between pattern elements, lessening constraint in their independent evolutionary trajectories (Beldade and Brakefield 2002; Beldade et al. 2002).

The common theme of butterfly wing evolution is called the "nymphalid ground plan" and was originally proposed by Schwanwitsch (1924) and Süffert (1927) who independently defined similar systems of positional homologies between pattern elements in Nymphalidae. Using Schwanwitsch's nomenclature, the major ground plan elements are as follows (fig. 1A): 1) "Basalis" (B), a hemi-pattern found at the root of the wing and that can be fully individualized in moths; 2) "Discalis II" (DII), a small symmetry system running anteroposteriorly between the radial and cubital veins, sometimes called "orbicular spot" in Noctuidae; 3) "Discalis I" (DI), or "discal spot," a small symmetry system always centered at the distal tip of the discal cell, where a discal crossvein usually joins the radial, median, and cubital veins. DI sometimes takes a rounded aspect, in which case it can be called a "discal ocellus," or, when it takes a bean shape, a "reniform spot"; 4) the two bands MII and MI, that form the large central symmetry system, generally centered on DI; 5) the "border ocelli" (Oc), commonly called "eyespots," which form concentric rings each centered equidistantly between two wing veins; 6) "Externae patterns" (E) are the parafocal, submarginal, and marginal elements (EIII, EII, and EI, respectively) that border the wing. As well, there are the vein-associated pattern elements (not shown): 7) *Venosa* (V), which occur along wing veins, and 8) *Intervenosa* (I), which occur midway between wing veins. No extant species exhibits the full ground plan, so it is best seen

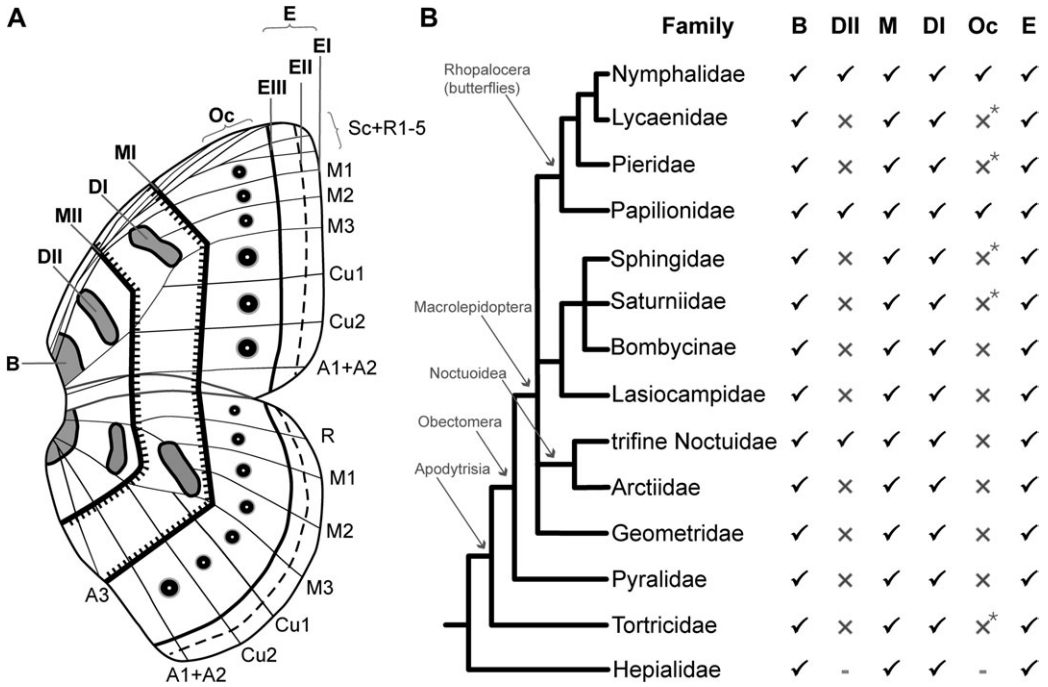

Fig. 1. The nymphalid ground plan across Lepidoptera. (*A*) Classical nymphalid ground plan with Schwanwitsch pattern nomenclature. (*B*) Phylogenetic spread of each ground plan pattern element across Lepidoptera. ✓: encountered in the clade; ✕: not encountered; - : not encountered after a noncomprehensive analysis only; asterisk: lycaenid and pierid butterflies sometimes form round-symmetry patterns reminiscent of Oc patterns but are positional homologs of E2 and E3, respectively (Schwanwitsch 1949, 1956b). Similarly, the border ocelli sometimes encountered in Saturniidae, in Sphingidae, in Noctuidae (e.g., *Opsigalea blanchardi*), or in Tortricidae (e.g., *Endopiza cyclopiana*) are best defined as E positional homologs. It was also proposed that Lycaenidae have true Oc elements and no EI-II (Nijhout 1991).

as the maximal arrangement of patterns elements encountered among nymphalids.

After its initial description, the nymphalid ground plan was extended to the wing patterns of butterfly families, such as Pieridae (Schwanwitsch 1956b), Lycaenidae (Schwanwitsch 1949), and Papilionidae (Süffert 1927; Schwanwitsch 1943), as well as to moth families including Saturniidae, Sphingidae, Noctuidae, Geometridae, Arctiidae, Pyralidae, and Tortricidae (Sokolov 1936; Henke and Krüse 1941; Schwanwitsch 1956a). When considered in the context of modern phylogenetic work, these early studies provide a working model for the evolution of the ground plan across the major families of Lepidoptera. We can infer from these studies a prototypical Lepidopteran ground plan consisting of a B pattern, a central symmetry system (MI-II), a discal spot (DI), and the EI–III elements (fig. 1*B*). Under the strict definition of positional homologies, Oc patterns are found only in Nymphalidae and Papilionidae (e.g., *Parnassius* spp.), but border ocelli sensu lato are also found in Lycaenidae, Pieridae, Saturniidae, Sphingidae, and Tortricidae (see fig. 1 legend). Finally, DII positional homologs have only been described in Nymphalidae, Papilionidae, and Noctuoidea.

Butterfly wing patterns are best defined as symmetry systems, meaning that their color fields are symmetrical relative to axial or focal sources of putative morphogens (Nijhout 1990, 2001). It emerges from developmental studies mainly focused on nymphalid Oc patterns that evolution within these pattern systems often results from variation in the number, shape, position, and downstream effect of these sources. Nymphalid Oc are induced by a focal source that pinches off from an ancestral I pattern signaling system, where the intervenous gene expression intersects with a presumed E prepattern (Reed and Serfas 2004). Generally, it has been proposed that the butterfly wing compartmental patterning system evolved via the co-option of genes classically involved in *Drosophila* wing development (Carroll et al. 1994). For instance, genes of the Hedgehog, Wingless, Notch, and transforming growth factor-*ß* pathways, as well as the transcription factors spalt, engrailed/invected, and Distal-less, all show expression patterns suggesting new functions related to wing color pattern development, in addition to expression patterns associated with the known functions of their *Drosophila* homologs (Carroll et al. 1994; Keys et al. 1999; Brunetti et al. 2001; Reed and Serfas 2004; Monteiro et al. 2006).

Most of the molecular work on lepidopteran wing pattern formation has thus far focused on gene expression during eyespot determination. Therefore, despite the intense interest in the evolution and development of lepidopteran wing patterns, very little is currently known about the molecular developmental basis of noneyespot ground plan elements. The only exceptions to this are a single reported *wingless* (*wg*) expression pattern correlated with DI and DII elements in a nymphalid butterfly (Carroll et al. 1994) and a report of engrailed/invected expression correlated with the DI discal spots of saturniid moths (Monteiro et al. 2006). *wg* gained further interest after it

was recently identified as the first known morphogen involved in animal color patterning (Werner et al. 2010). Unfortunately, however, many gaps remain in our understanding of noneyespot lepidopteran wing patterns.

In this study, we present a broad comparative analysis of the development and evolution of discal spot (DI) and basal symmetry system (DII) patterns across Lepidoptera. In addition to confirming and significantly expanding upon the previous report of *wg* expression in DI and DII, we also describe a novel Lepidoptera-specific homeobox transcription factor, *aristaless2* (*al2*), which temporally precedes *wg* in DII-specific expression patterns. We further present an extensive cross-species comparison of *wg* and *al2* expression patterns in the context of lepidopteran phylogeny and color pattern evolution in order to make inferences regarding the origin, evolution, and developmental homologies of the DI and DII elements in Lepidoptera. Together, our findings paint a substantially expanded portrait of the origin and evolution of several major elements of the nymphalid ground plan.

Materials and Methods

Review of Existing Literature

Classic work on the derivation of the nymphalid ground plan was used to determine positional homologies among wing patterns of various Lepidoptera families (for references, see Introduction). Presence/absence of a pattern element in each clade was confirmed by screening wing diversity using the online databases www.barcodinglife.org, www.tortricidae.com, and mothphotographersgroup.msstate.edu and printed resources (Seitz 1906; Smart 1991). The character matrix shown in figure 1*B* summarizes the synthesis of Schwanwitsch (1956a) with the following modifications: 1) B was used to define the basal symmetry system as a whole rather than its distal boundary alone; 2) the Discalis III element (DIII) was omitted because it was observed by Schwanwitsch only in Pyralidae (e.g., *Nymphula nymphaeata*) and is probably a modified circular B element; and 3) the moth elements Terminalis, Terminal Umbra, and Externa were considered as positional homologs of the parafocal (EI), submarginal (EII), and marginal (EIII) Externae of the nymphalid ground plan, respectively. In addition to these clarifications, we provided two major additions for the purpose of this study: 1) the derivation of some of the ground plan elements was extended to the Hepialidae and the saturniid subfamily Bombycinae; for instance, a clear DI is found under the form of a discal ocellus in *Zelotypia stacyi* (Hepialidae) and 2) while Schwanwitsch presented a tortricid ground plan devoid of DI, we changed this after observing examples of unambiguous tortricid DI positional homologs (e.g., *Meritastis polygraphana*).

Distribution of DI and DII Pattern Elements

To assess the distribution of the DI and DII elements, the online collections of the North American Photographers Group (mothphotographersgroup.msstate.edu, Mississippi Entomological Museum) and tortricid.net (www.tortricidae.com, Colorado State University) were used as sources of wing photographs for non-Rhopalocera lepidopterans. For Rhopalocera, we referred to Smart (1991). Some of the moth species were reclassified in their proper family/superfamily according to the Catalogue of Life 2009 (Bisby et al. 2009). Presence of a pattern was called only in unambiguous cases, in such a way that our data may potentially contain false negatives (e.g., when DI or DII are masked by the central symmetry system, or when these patterns are only visible on the ventral side) but virtually no false positives. DI elements were, by definition, easily recognizable due to their placement on the discal crossvein. DII elements were sometimes more difficult to identify than DI elements. On the anteroposterior axis, both are limited by the radial and cubital veins, but DII elements have no precise proximodistal landmark. Particular care was taken to avoid the confusion of DII elements with broken or dislocated MII bands, and in some cases, unambiguous DII identification in one species allowed a secondary identification in closely related species. Also, our moth (non-Rhopalocera) samples mainly consisted of Nearctic species, but this geographic bias did not appear to result in a significant phylogenetic bias, as testified by good sampling at the subfamily level.

Phylogenetic Reconstruction

The CONSENSE module of the PHYLIP package (Felsenstein 1989) was used to make a strict consensus tree of Lepidoptera families based on previously published phylogenies. The Lepidoptera phylogenetic backbone was taken from Kristensen et al. (2007). Deeper level phylogenetic relationships were obtained from molecular phylogenies within Rhopalocera (Wahlberg et al. 2005; Pohl et al. 2009), the Lasiocampidae–Bombycoidea complex (Regier et al. 2008), and the Noctuoidea complex (Lafontaine and Fibiger 2006; Mitchell et al. 2006).

For gene phylogenies, protein sequences were aligned with MUSCLE (Edgar 2004). Nucleotide GenBank accession numbers are as follows: *Aedes egypti Ae_al* XM_001649303; *Anopheles gambiae Ag_al* XM_317481; *Apis mellifera Am_al* XM_624627; *Bicyclus anynana Ba_al2* GE712158; *Culex quinquefasciatus Cq_al* XM_001861999 + XM_001862000; *Drosophila melanogaster Dm_al* NM_164382 and *Dm_hbn* NM_176240; *Drosophila virilis Dv_al* XM_002052787; *Harmonia axyridis Ha_al* AB200970; *Heliconius erato He_al2* GU263417 and *He_al1* GU263418; *Junonia coenia Jc_al1* GU263416 and *Jc_al2* GQ478705; *Nasonia vitripennis Nv_al* XM_1607662; *Pediculus humanus Ph_al* XM_002432402; and *Tribolium castaneum Tc_al* NM_1114366. *Bombyx mori Bm_al1*, *Bm_al2*, and *Daphnia pulex Dp_al* sequences were deduced from TBlastN searches in SilkDB and WFleaBase. Start to stop codon intervals were retrieved from their corresponding genome sequence databases using the following coordinates: *Bm_al1* nscaf2847:3796930 . . . 3818394; *Bm_al2* nscaf2847:3963864 . . . 3972542 + nscaf797:1 . . . 7386; and *Dp_al* scaffold_11:130080 . . . 132933. The homeodomain region, the C-terminal OAR domain, and two other regions of al proteins

were unambiguously aligned (supplementary fig. S1, Supplementary Material online). After gap removal, a concatenated alignment of these amino acid sites was used as a guide for nucleotide alignment using PAL2NAL (Suyama et al. 2006). The third nucleotide position of each codon was removed. Maximum likelihood (ML) and Bayesian inference (BI) phylogenetic analysis were carried out using PHYLIP and MrBayes (Felsenstein 1989; Ronquist and Huelsenbeck 2003). Addition of *B. anynana* and *J. coenia* sequences resulted in an identical tree topology with lower branch support due to the loss of informative sites. RRTree was used to perform relative-rate tests between the Lepidoptera *al1* and *al2* branches using non-lepidopteran Holometabola sequences as an outgroup (Robinson-Rechavi and Huchon 2000).

Animals

The origin and rearing conditions for each species are presented in supplementary table S1 (Supplementary Material online). Larvae were anaesthetized at −20 °C and dissected in cold phosphate-buffered saline (PBS) during the last larval instar. In butterfly species, the developmental sampling covered the main stages of wing disk development that are defined according to tracheal differentiation (Reed et al. 2007). Moth wing disks were staged more roughly according to the following chart (with nymphalid-equivalent stages between parenthesis, for comparison): early = no tracheal differentiation (Stage 0–0.75), mid = tracheae are introgressing into the vein lacunae until they reach the border lacuna (Stage 1–2), and late = trachea is invading the border lacuna (Stage 2.25–3). To maximize the developmental sampling of moth species, most caterpillars were dissected between 0 and 2 days after they stopped feeding (wandering stage), an event that marks the beginning of tracheal differentiation in *Manduca sexta* (Nijhout et al. 2007). Sampling covered the early and mid stages in every moth species (supplementary table S1, Supplementary Material online). Late stage moth disks were rarely obtained, yet they always presented faint *al2* expression, an observation that is similar at equivalent stages in butterflies. Dissection of wing anlagen from the beetle *Zophobas morio* was possible only 2 days after the larvae adopted a hook posture (Quennedey and Quennedey 1999).

Molecular Cloning and Probe Synthesis

A *J. coenia* (*Jc*) first-strand cDNA pool was synthesized from fifth instar and pupal wing total RNA using M-MLV reverse transcriptase (Promega). Partial *Jc_al1* and *Jc_al2* cDNAs were amplified using a Touchdown polymerase chain reaction (PCR) protocol and degenerate primers targeting overlapping regions of each transcript (*Jc_al1_F1* 5′-ATCAGAAGTNCCNAARGAYGA, *Jc_al1_R1* 5′-TGTGAGAAGGGGTTGGGCAT, *Jc_al1_F2* 5′-CGCACCCGTAYAAYCCNTAY, *Jc_al1_R2* 5′-CAACTAATTAGRTCNGTRTGRTG, *Jc_al2_F1* 5′-GTGGGATGGAYGAYGARGAYAT, *Jc_al2_R1* 5′-TCCGCTGTACGGATGTGCG, *Jc_al2_F2* 5′-GGIAGIACGCATTATCCTGATGT, *Jc_al2_R2* 5′-GGIGGIAGGTAC TGTGCICC, *Jc_al2_F3* 5′-GGCGGGCAGCCATTGCCAAC, *Jc_al2_R3* 5′-GCKATRCTSGAACTYCTWACATC). To produce paralog-specific riboprobes, the *Jc_al1_F2-R2* and *Jc_al2_F3-R3* fragments were used due to low conservation in the 3′-region (supplementary fig. S1, Supplementary Material online). Partial *Jc_wg* was amplified using the WG1 and WG2 primers (Brower and DeSalle 1998). Fragments were cloned in the pCRII vector (Invitrogen) and sequenced on both strands before digoxigenin-labeled riboprobe synthesis (Roche AS). The *Jc_wg* riboprobe cross-hybridized efficiently in every species considered.

Immunohistofluorescence and In Situ Hybridizations

Immunohistofluorescence was carried out using a previously described protocol (Brunetti et al. 2001). The primary antibody DP311 (1:20 dilution) was detected with Cy3 goat anti-mouse secondary antibodies (Jackson Immunoresearch), and tissue samples were counterstained with the nuclear marker 4′,6-diamidino-2-phenylindole. Most moth species required dissection of the peripodial membrane after fixation to allow efficient staining. In situ hybridizations were performed as described previously (Carroll et al. 1994; Reed and Nagy 2005) with the exception that riboprobes were incubated with the tissues at 65 °C instead of 55 °C and that we were able to use wing disks stored at −20 °C in methanol after progressive dehydration and rehydration.

For the double detection of *al2* and *wg*, *J. coenia* wing disks were dissected in PBS, fixed 30 min on ice with 9% formaldehyde, washed, incubated 45 min with DP311 at 4 °C, quickly washed (3 × 2 min), incubated 30 min with the DyeLight488 rabbit anti-mouse secondary antibodies (Jackson Immunoresearch), quickly washed, and postfixed 20 min on ice with 4.5% formaldehyde. The blocking step was omitted due to possible RNAse activity of bovine serum albumin. In situ hybridization was then carried out normally without proteinase K digestion step. For fluorescent detection of *wg* transcripts, one Fast Red tablet was dissolved in 2 ml of 0.1 M Tris–HCl pH8.2, 0.1% Tween 20, filtrated, and incubated with the tissues in the dark until the appearance of red precipitate. All tissue samples were visualized and digitally photographed on a fluorescent transmission light microscope. All fluorescent imaging was combined with phase contrast imaging in order to visualize wing venation (e.g., supplementary fig. S4, Supplementary Material online).

Results

DI Elements Are Widespread Across Lepidoptera While DII Shows a Scattered Distribution

The existing literature assigns nymphalid ground plan elements to many of the wing patterns found throughout Lepidoptera (fig. 1). DI and DII in particular appear to have many positional homologs outside of Nymphalidae and Rhopalocera, yet it has been unclear to what extent these elements are conserved or convergent across other lepidopteran lineages. To clarify this issue, we screened for

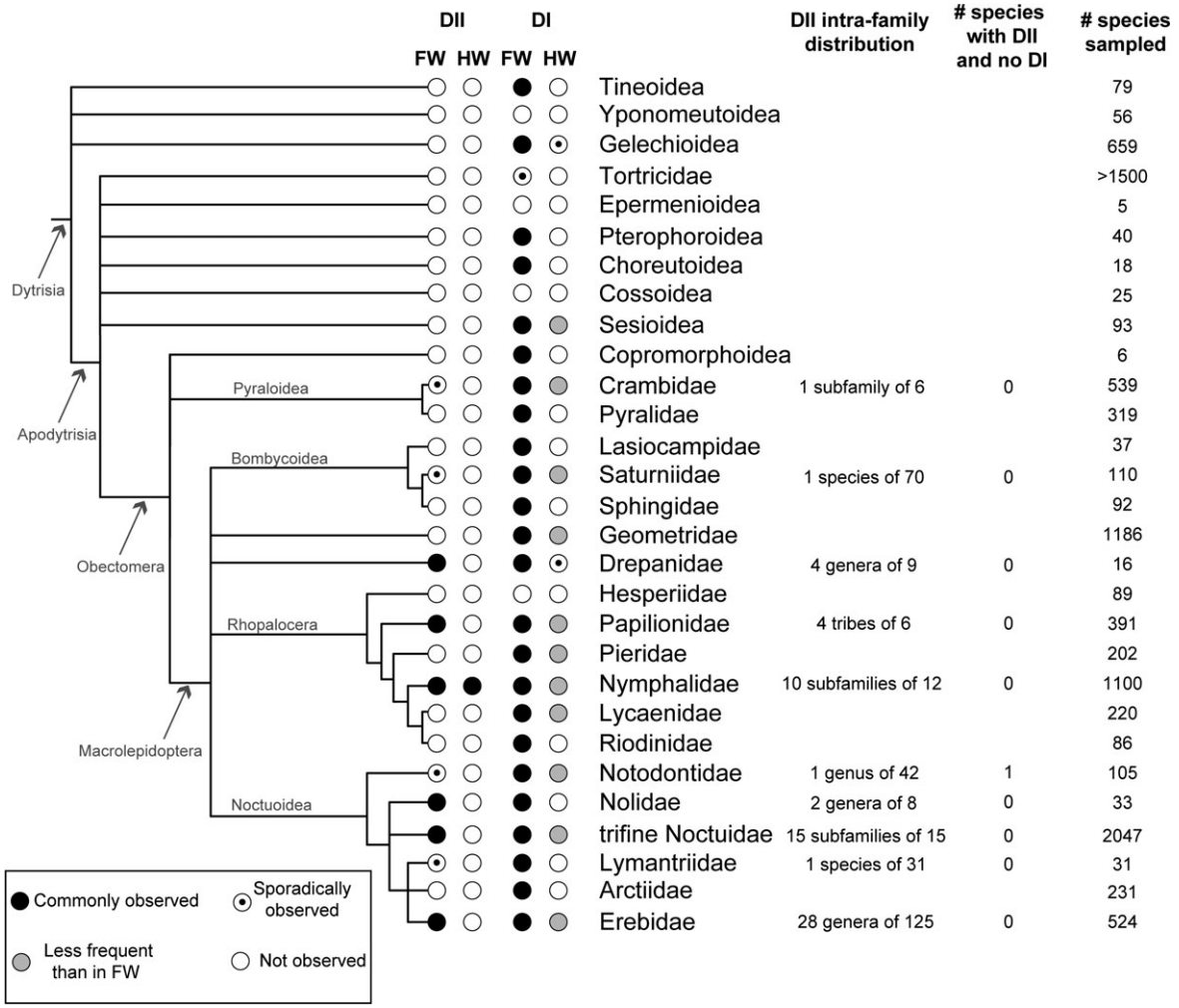

Fig. 2. Phylogenetic distribution of DII and DI elements. Consensus phylogeny of Lepidoptera featuring the distribution of DII and DI elements in forewings (FW) and hindwings (HW). For details, see supplementary table S2 (Supplementary Material online).

the presence of DI and DII elements in dorsal wing patterns of approximately 9,000 species spanning 29 of the most speciose families of Lepidoptera and mapped character absence/presence on a consensus phylogeny (fig. 2, supplementary table S2, Supplementary Material online). We found many examples of forewing DI elements in every family we sampled, with the exception of a handful of clades with small sample sizes (Epermenioidea, Cossoidea) or in families where DI is potentially masked by other patterns (Yponomeutoidea, Hesperiidae). Hindwing DI elements were primarily observed in Obectomera and were always less frequent in hindwings than in forewings. This observation also remained true outside of Obectomera, where hindwing DI elements appeared in a fraction of Sesioidea species with a forewing DI (e.g., *Synanthedon acerni*).

When considering forewings, DII elements had a much more scattered distribution than DI. Outside of Macrolepidoptera, we observed them in only a single subfamily (Pyraustinae, Crambidae). In Macrolepidoptera, DII elements were found sporadically (i.e., in only one species or genus) in Lymantriidae, Notodontidae, and Saturniidae. They were common, but often reduced, in Drepanidae, Nolidae, and Erebidae, and were nearly ubiquitous, and usually well developed, in Papilionidae, Nymphalidae, and trifine Noctuidae. In hindwings, DII were only found in Nymphalidae. Regardless of the wing or taxon considered, DII elements were always less frequent than DI. We also observed that DII elements were never observed in the absence of DI, with the possible exception of a single species, *Datana integerrima* (Notodontidae).

wg Marks the Development of Major Ground Plan Elements in Larval Wing Disks

We reproduced and extended the previous observation that *wg* marks the development of DI and DII in the nymphalid *J. coenia* (Carroll et al. 1994) in fifth-instar wing disks (fig. 3A–H). We found that in early stages (Stage 0–0.5), *wg* is primarily expressed in the peripheral tissue and wing hinge, eventually becoming expressed in the presumptive DII pattern element, followed by the DI element. After stage 0.75, the peripheral tissue expression extends into the wing tissue, forming two fingers that flank the midline and that could be associated with patterning of the EI-EII elements (Carroll et al. 1994). We also found that the

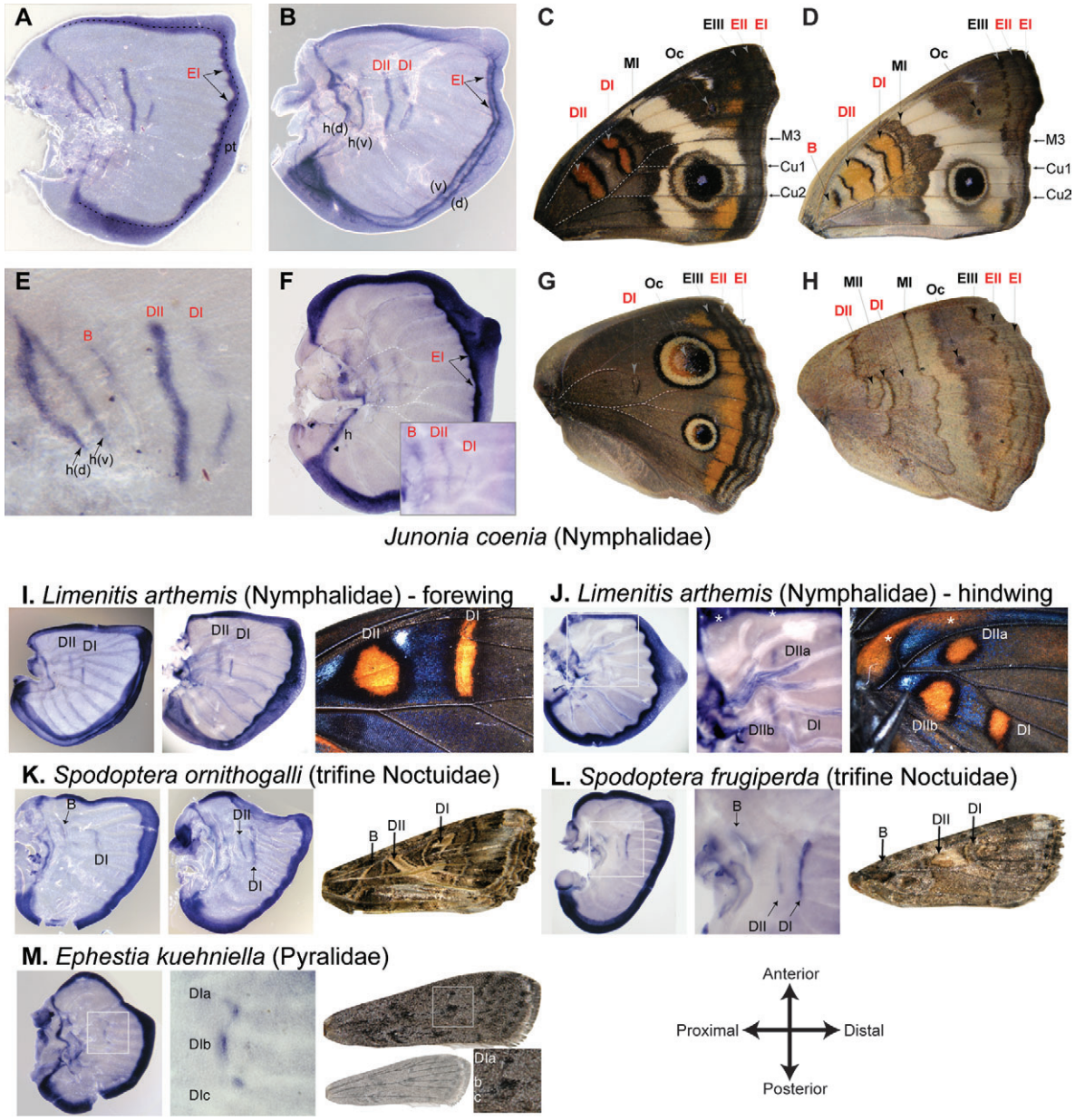

Fig. 3. Last-instar wing disk expression of *wg* throughout Lepidoptera. (*A–B*, *E–F*) *wg* expression in *Junonia coenia* in stage 1.5 (*A* magnified in *E*), stage 2.5 (*B*) fifth-instar forewing, and stage 2.0 fifth-instar hindwing (*F*). Red, expression in presumptive pattern elements; black dotted line, wing margin; pt, peripheral tissue; h(v) and h(d), ventral and dorsal sides of the wing hinge; (v) and (d), ventral and dorsal sides of the wing margin. (*C*, *D*) dorsal and ventral *J. coenia* adult forewing; (*G*, *H*) dorsal and ventral *J. coenia* adult hindwing; Red, elements predicted to be patterned by a heparin-sensitive morphogenetic substance (Serfas and Carroll 2005); black, other pattern elements. (*I–J*) *wg* expression in *Limenitis arthemis* corresponds to orange–black pattern elements of the ventral forewing and hindwing. Stage 2.0 and stage 3.0 forewings (H, left and middle); stage 2 hindwing (I, left and magnification); *, costal orange element. (*K–L*) *wg* prepatterns B, DII, and DI elements in the *Spodoptera* genus forewings; mid (left) and late (middle) *Spodoptera ornithogalli* forewings (*K*); mid *S. frugiperda* forewing (*L*); (*M*) *wg* prepatterns DI in *Ephestia kuehniella*; mid forewing (left and magnification).

forewing B element is prepatterned by *wg* expression (fig. 3*A* and *E*). What results from these observations is that presumptive B, DII, DI, and EI color pattern elements of *J. coenia* are likely sources of the wg signaling molecule.

wg expression was assessed in last-instar wing disks of *Limenitis arthemis* (Nymphalidae), *Spodoptera ornithogalli* and *Spodoptera frugiperda* (trifine Noctuidae), and *Ephestia kuehniella* (Pyralidae) (fig. 3*I–M*). Similar to the association of *wg* expression with the orange-and-black stripe patterns seen in *J. coenia* (fig. 3*A–E*), DI and DII *wg* expression was observed in both forewings and hindwings of the nymphalid *L. arthemis* (fig. 3*I–J*). In tight association with the adult pattern, the hindwing DII *wg* expression is disrupted by the radial veins into two separate pattern elements. Also, *L. arthemis* wings lack obvious B elements, but hindwings bear a costal/basal orange pattern whose shape approximately corresponds to a domain of *wg* expression. It is noteworthy that DI *wg* expression in this species occurs

even in the absence of discal crossveins in hindwings, implying a role for *wg* in color pattern formation independent of wing vein determination. Outside of Nymphalidae, DI-associated *wg* expression was remarkably conserved in noctuid and pyralid forewings (fig. 3*K*–*M*). As in nymphalids, both noctuid species showed a stripe of *wg* expression in their presumptive DII elements and a basal domain of expression possibly representing a cryptic B element. The noctuid and pyralid hindwings we analyzed were devoid of patterns and showed only peripheral expression of *wg* (data not shown). In *Battus philenor* (Papilionidae), both wings lack central color pattern elements and, here again, *wg* expression was not observed in the wing field (McDonald et al. 2010).

al Is Duplicated in Lepidoptera

We were interested in identifying additional genes besides *wg* involved in DI and DII patterning. Preliminary immunochemistry results (see below) suggested a possible DI/DII patterning role for one or more Pax3/7 paired-class homeodomain proteins, which are a family of transcription factors that includes *al*. While collecting Lepidoptera *al* sequences, we found that *al* was tandemly duplicated in the *B. mori* genome assembly (fig. 4*C*). We subsequently cloned and characterized *aristaless1* (*al1*) and *aristaless2* (*al2*) from *J. coenia* larval wing disk cDNA and identified them from wing disk transcriptome and preliminary genome sequences of the nymphalids *H. erato* and *Heliconius melpomene*, respectively (fig. 4*A*–*B*, data not shown). While both *al* paralogs were consistently found in lepidopterans, only one copy of *al* was found in genome and transcriptome sequence databases of non-lepidopteran insects, suggesting that the *al* duplication is Lepidoptera specific. In support of this idea, phylogenetic reconstruction of *al* sequences using ML and BI places the *al* duplication event within the Lepidoptera lineage, before the Bombycoidea–Rhopalocera split (fig. 4*C*).

Accelerated Rate of Evolution in the *al2* Coding Region after Duplication

Phylogenetic reconstruction of *al* sequences based on first and second nucleotide positions (fig. 4*D*) resulted in a tree with a strikingly long *al2* clade branch. Because changes in first and second positions are often nonsynonymous, we hypothesized this acceleration might be related to the observed fixation of amino acid substitutions in al2 (fig. 4; supplementary fig.S1, Supplementary Material online), notably in the homeodomain (DNA-binding) and OAR domain (for *otp-aristaless-rax*, function unknown). To test for *al2* coding divergence following the *al* duplication, we performed a phylogenetically weighted relative-rate test implemented in the program RRTree (Robinson-Rechavi and Huchon 2000) and compared the rates of nonsynonymous substitutions (K_a) in the lepidopteran *al1* and *al2* sequences compared with the non-lepidopteran holometabolan *al* sequences. The differences between *al1* and *al2* branch K_a values were significant when analyzing the whole data set ($P < 0.002$) and the homeodomain only ($P < 0.01$) but not the OAR domain ($P > 0.4$). Therefore, *al2* underwent significant divergence at coding sites, an asymmetrical divergence that is not observed among other *al* lineages. Saturation of nucleotide substitutions in the data set hindered the possibility to compute K_s values in order to test for directional selection at these sites.

al1 and *al2* Underwent *Cis*-Regulatory Divergence after Duplication

In addition to coding sequence comparisons, we also compared *al1* and *al2* expression patterns in the nymphalid *J. coenia* using in situ hybridization of paralog-specific riboprobes (fig. 5*A* and *E*). To control for variability in developmental stages, the left and right wings of the same fifth-instar individuals were each stained for a different paralog and compared. Strikingly, the two paralogs showed divergent expression patterns with little overlap. *al1* was observed in two discrete domains of the anterior compartment: the wing costa (anterior wing margin) and an expression domain starting at the root of the radial tracheal trunk and extending proximo-distally to the R4-5 tracheal branch (fig. 5*A*). In contrast, *al2* expression was revealed in a narrow stripe of expression that extends anteroposteriorly between the roots of the radial and cubital tracheal trunks (fig. 5*E*). Therefore, *al1* and *al2* acquired different expression domains in the wing disk after duplication, a process known as *cis*-regulatory divergence.

The DP311 Antibody Detects al1 and al2 during Wing Development

We wanted to compare *al2* expression in a variety of species; however, a strategy based on in situ hybridization of transcripts would have involved significant technical challenges, including cloning and generating riboprobes for *al2* in multiple species, preserving endogenous transcripts in a large number of samples and relatively low sensitivity and high experimental variability. Therefore, we used an antibody-based strategy to detect al2 proteins across taxa. During a screen for the cross-reactivity of *Drosophila* monoclonal antibodies in *J. coenia* imaginal disks, we found that the Pax3/7 DP311 monoclonal antibody (Davis et al. 2005) produced a signal that recapitulates *al1* and *al2* expression (in particular, see fig. 5*C*). Another antibody, DP312, also designed to target paired-like family homeodomains, did not produce any signal in *J. coenia* wing disks. This difference of reactivity was characterized as the signature of an *F* residue at position 31 of the *Drosophila* homeodomain (Davis et al. 2005). Because the DP311 epitope and the F_{31} residue are conserved in all the insect al protein sequences (fig. 4*A*), we thus confirmed that the DP311 antibody specifically recognizes both *al1* and *al2* proteins during wing development. This being the case, we were justified in using DP311 as a marker to investigate the expression of *al1* (DP311/*al1*—anterior margin and radial trachea) and *al2* (DP311/*al2*—anteroposterior stripe) expression patterns across taxa.

In addition to recapitulating the *al1*/*al2* expression pattern, large DP311-positive cells were additionally found in the basal tracheal masses of the wing disks. These cells

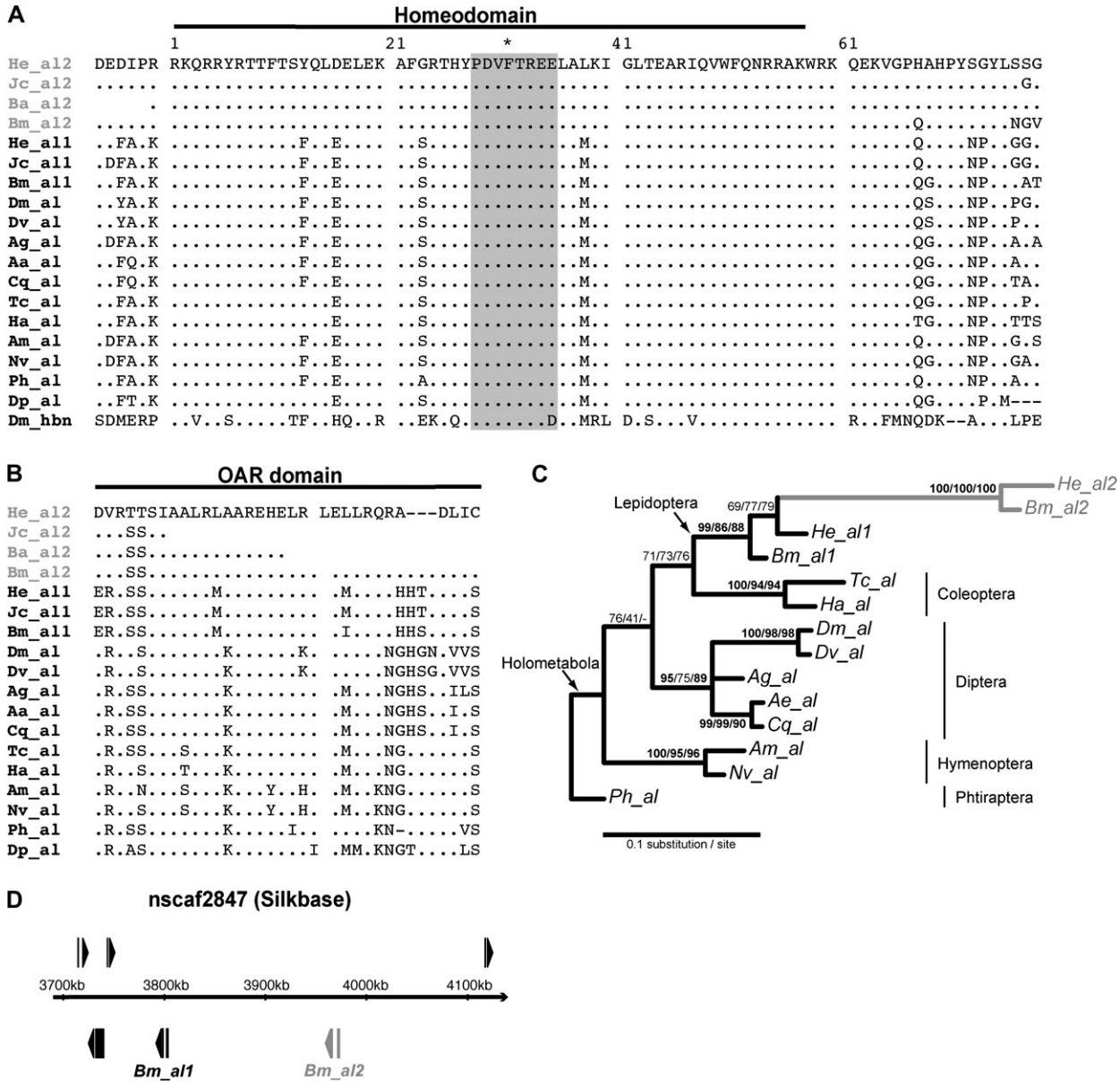

Fig. 4. *al* duplication in Lepidoptera. (*A*) Alignment of insect al homeodomains. *Daphnia pulex* al (Dp_al) and *Drosophila melanogaster* homeobrain (Dm_hbn) are used as outgroups. The DP311-specific epitope is highlighted, with the F_{31} residue not recognized by the DP312 antibody (asterisk). (*B*) Alignment of insect al OAR domains. (*C*) Phylogenetic reconstruction of holometabolan *al* nucleotide sequences using BI. Identical topology was obtained using the ML method. Statistical confidence in nodes is expressed as BI bootstrap support/ML bootstrap support/ML approximate likelihood-ratio test value. (*D*) Genomic annotation in the *Bombyx mori al1/2* region (SilkDB, contig nscaf2847); *al* is tandem duplicated, and both copies are the only annotated genes in a 350 kb wide region. Aa: *Aedes aegypti*; Ag: *Anopheles gambiae*; Am: *Apis mellifera*; Ba: *Bicyclus anynana*; Bm: *B. mori*; Cq: *Culex quinquefasciatus*; Dm: *D. melanogaster*; Dp: *D. pulex*; Dv: *Drosophila virilis*; Ha: *Harmonia axyridis*; He: *Heliconius erato*; Jc: *Junonia coenia*; Nv: *Nasonia vitripennis*; Ph: *Pediculus humanus*; and Tc: *Tribolium castaneum*.

begin to occur along the wing lacunae after stage 2, highlighting the position of future wing veins. Interestingly, only the veins that persist in the adult wings contain DP311-positive cells (fig. 5*D* and *H*), and this pattern is maintained during pupal stages (data not shown). These cells are possibly future sensory cells dispersed along the wing veins, which are known to differentiate as early as tracheal invasion in fifth-instar disks (Galant et al. 1998). Because neither *al1* nor *al2* transcription was detected in these large tracheal cells, these cells probably express an unidentified Pax3/7 family homolog bearing the F_{31} residue.

The DP311/*al2* Stripe Prefigures *wg* DII Expression

To test for the possible involvement of *al2* stripe expression in nymphalid ground plan development, we assessed the position of the anteroposterior stripe of DP311/*al2* expression relative to the DII and DI pattern elements in *J. coenia* wing disks (fig. 5*I*–*K*). DP311/*al2* stripe expression was detectable as early as stage 0, preceding the establishment of DII *wg* expression. *wg* expression was detectable after stage 1.25, and a codetection assay showed that the DII domain of *wg* expression coincides with the narrow domain of DP311-positive cells, between the radial and cubital

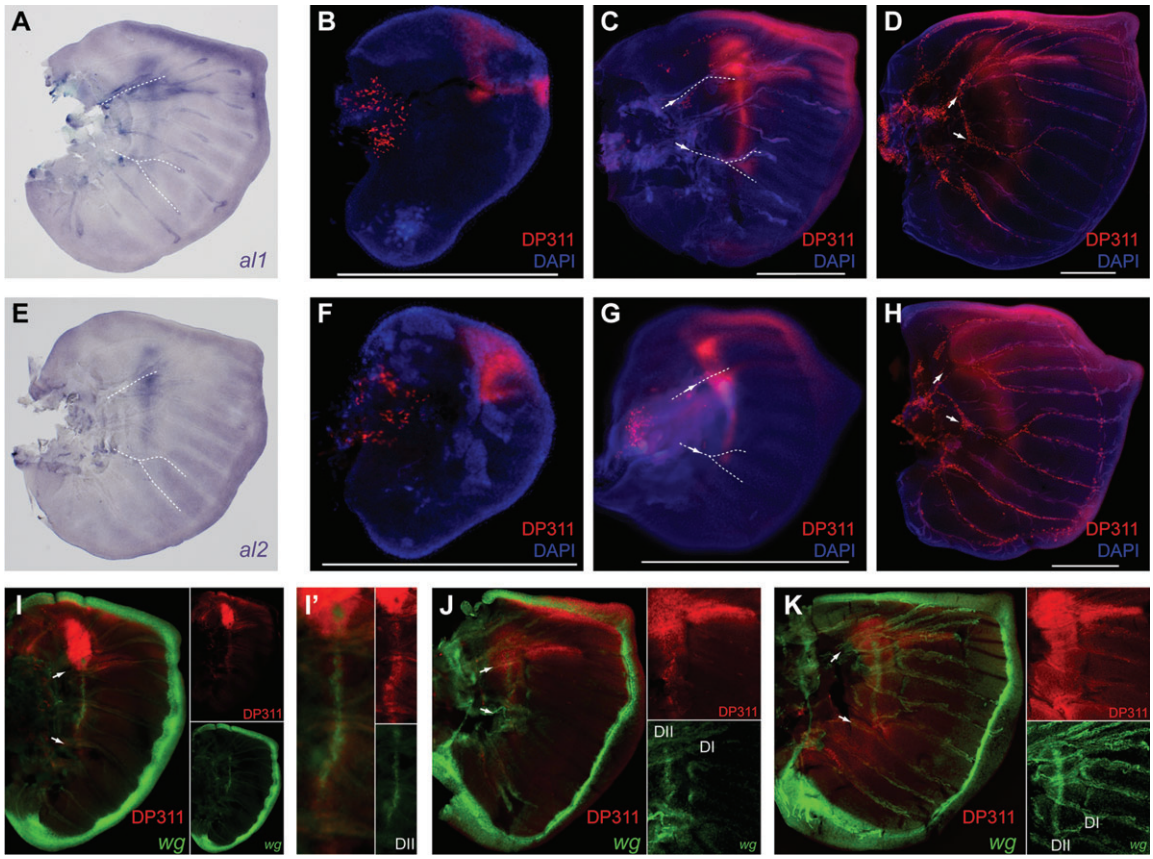

Fig. 5. Expression of *al1* and *al2* in *Junonia coenia* wing disks. (*A*–*B*) mRNA expression of *al1* and *al2* in a single individual at stage 1.5. The right forewing (*A*) and the mirror image of the left forewing (*B*) are shown. The tracheal staining in (*A*) is commonly observed with many probes and is most likely due to nonspecific probe binding. (*C*–*E*) Expression of the DP311 antigen in fourth instar (*C*), stage 1.5 (*D*), and stage 2.5 (*E*) fifth-instar forewings, counterstained with 4′,6-diamidino-2-phenylindole (DAPI) (blue). (*F*–*H*) Expression of the DP311 antigen in fourth (*F*), stage 1.25 (*G*), and stage 2.5 (*H*) fifth-instar hindwings, counterstained with DAPI (blue). (*I*–*K*) Codetection of the DP311 antigen (red, immunofluorescence) and of *wg* mRNA (green, fluorescent in situ hybridization) at stage 1.25 (*I*, magnified in *I*′), stage 2.0 (*J*), and stage 2.5 (*K*) fifth-instar forewings. White arrows and dotted lines indicate the position and axis of the radial (anterior) and cubital (posterior) tracheal trunks. Scale bars = 0.5 mm.

tracheal trunks where the adult DII element occurs. While at this time point, the zone of DP311/*al2* expression is broader than the zone of *wg* transcription, when *wg* expression first appears the overlap with DP311/*al2*-positive cells appears to be very precise (fig. 3*I*′). Overall, these results suggest that *al2* may reflect early positional information for DII patterning upstream of *wg* expression.

The DP311/*al2* Stripe Is Ancestral in Forewings and Nymphalid-Specific in Hindwings

al2 expression is the earliest known event in DII patterning, and we sought to assess its last-instar expression pattern in nine lepidopteran families and one coleopteran outgroup. Because of its sensitivity and versatility, DP311 antibody staining was preferred to in situ hybridization to test for an association of *al2* expression in the context of DII evolution (supplementary figs. S2 and S3, Supplementary Material online). Thusly, we focused our comparative work on the DP311/*al2* pattern—the region of DP311 antigenicity between the radial and cubital tracheal trunks (position and axis indicated by arrows in the figures).

In forewings (supplementary fig. S2, Supplementary Material online), we found three categories of correlation between DP311/*al2* expression and the adult patterns. 1) The DP311/*al2* antigen was detected as a continuous stripe in families in which DII is common: Nymphalidae (*J. coenia*, *L. arthemis*, *Agraulis vanillae*, and data not shown for *Vanessa cardui*, *Nymphalis antiopa*, and *Heliconius* spp.), and Noctuidae (*S. ornithogalli* and *Pseudoplusia includens*). A faint but reproducible pattern of continuous expression was also observed in a papilionid (*B. philenor*). Of the aforementioned species, only *J. coenia*, *L. arthemis*, *A. vanillae*, *V. cardui*, *S. ornithogalli*, and *P. includens* have a DII element. 2) The DP311/*al2* antigen was detected as a continuous stripe in families in which DII is absent: Bombycoidea (*B. mori* and *M. sexta*), Pyralidae (*E. kuehniella*), and Tortricidae (*Cydia pomonella*). 3) The DP311/*al2* antigen was detected as discontinuous domains in families in which DII is absent: Pieridae (*Pieris rapae*) and Geometridae (*Disclisioprocta stellata*). In these species, the DP311 antigen had two foci of expression at the roots of the radial and cubital tracheal trunks, with no expression in between.

In hindwings (supplementary fig. S3, Supplementary Material online), DP311/*al2* expression correlated with DII presence at the family level. Indeed, all the considered species showed a discontinuous expression domain between the radial and cubital tracheae, whereas all the nymphalid species exhibited a stripe of expression regardless of the presence or absence of DII in adults (*J. coenia*, *L. arthemis*, and data not shown for *V. cardui*, *N. antiopa*, and *Heliconius* spp.).

When considering both forewings and hindwings, some of the features of DP311 antigenicity described above in *J. coenia* were retrieved across Lepidoptera. In every species considered, the DP311 antibody produced the DP311/*al1* anterior compartment staining that remained particularly intense in the anterior costa and at the root of the radial tracheal trunk (fig. 5*H*). The tracheal giant cell staining which is not attributable to *al1* or *al2* expression was widely observed, particularly at the latest stages.

Variation in DP311/*al2* Expression across Taxa

Additional subtle variations in DP311 antigen expression were observed. 1) In *L. arthemis* (Nymphalidae), the DP311/*al2* stripe consisted of multiple individualized foci, especially at early stages. In hindwings, the DP311/*al2* stripe showed a breakage correlated with DII dislocation in the adult wing pattern, consistent with the theory that butterfly wing stripe patterns can be developmentally dislocated into multiple independent pattern elements (Nijhout 1994). 2) In *L. arthemis*, *S. ornithogalli*, *D. stellata*, *E. kuehniella*, and *C. pomonella*, DP311 signal extended into the anal region (posteriorly to the cubital trunk), usually in the form of an isolated spot (except in *L. arthemis*, where it was more stripe like). 3) In Noctuidae forewings, the DP311 antigen was expressed along the distal midline of every wing cell, a feature reminiscent of the pattern-associated expression of Distalless and Notch in other families (Reed and Serfas 2004). 4) DP311 antigenicity correlated with two pattern elements of the *Heliconius cydno galanthus* ventral hindwing (supplementary fig. S4, Supplementary Material online). Most *Heliconius* patterns are thought to derive from the nymphalid ground plan (Nijhout and Wray 1988) but the anterior component of the forcep-shaped red pattern does not express *wg*, arguing against DII homology (data not shown). This possible implication of *al1*/2 in patterning the costal element and the anterior component of the forcep pattern would be consistent with the genetic evidence that the *H. cydno galanthus* ventral hindwing is a composite assembly of independent colored and melanic patterns (Gilbert 2003; Naisbit et al. 2003; Kronforst et al. 2006).

Outside of Lepidoptera, the coleopteran last-instar wings and elytra only showed costal DP311 staining, reminiscent of the costal *al1* expression in *J. coenia* as well as intense signal in giant tracheal cells.

Discussion

Origin of a Wing Pattern Gene: Duplication and Neofunctionalization of *al* in Lepidoptera

In addition to the evidence that *al* underwent a tandem duplication in Lepidoptera, our data suggest that *al2* acquired new functions after the duplication event. First, *al2* underwent a relaxation of constraint at the coding level, as evidenced by the fixation of nonsynonymous substitutions at positions that are invariable in *al*/*al1* (fig. 4*A*–*B*, supplementary fig. S1, Supplementary Material online). This asymmetric divergence may reflect functional changes in domains important for posttranslational regulation, protein–protein interaction or, more importantly, might imply novel transcriptional targets, as suggested by the significant divergence of the homeodomain. It is also possible, however, that these changes were due to neutral evolution during a phase of relaxed functional pressure. Unfortunately, the large evolutionary distances considered in this study prevented us from using tests for positive selection that could rule out neutrality.

A second and more significant line of evidence for *al2* neofunctionalization comes from the difference in expression with *al1* during wing development. The nymphalid *al1* retained a costal and anterior compartment expression reminiscent, respectively, of coleopteran and dipteran *al* expression (fig. 6 and supplementary fig. S2, Supplementary Material online; Campbell et al. 1993; Campbell and Tomlinson 1998), suggesting that *al1* retained ancestral functions in wing disk development. In contrast, *al2* is expressed in a novel, Lepidoptera-specific anteroposterior stripe domain that introgresses into the posterior compartment. This case of *cis*-regulatory divergence joins several examples of duplication followed by expression difference and functional divergence of insect transcription factors (Wittkopp 2006). Finally, by analogy with the nymphalid expression patterns of *al1* and *al2*, the presence of a continuous stripe of DP311 antigen expression in Tortricidae and Pyralidae corroborates with an *al2* neofunctionalization episode prior to the Apodytrisia radiation. Because of the polyvalence of DP311, we cannot absolutely exclude the possibility that the DII-associated expression in moths is produced by *al1* or a combination of *al1* and *al2*. If this scenario were the case, however unlikely, it would represent an even more radical example of *cis*-regulatory divergence in the lepidopteran *al* genes than what we propose here. In the future, it will be interesting to get a more detailed view of this event by looking at *al1* versus *al2* expression in Trichoptera and basal lepidopterans. Taken together, these findings suggest that *al* underwent duplication after the Diptera/Lepidoptera split and that the *al2* copy was under functional relaxation and underwent neofunctionalization, at least by acquisition of a new expression domain characterized by stripe expression in last-instar wing disks.

Potential Roles for *wg* and *al2* in Wing Pattern Development

In a previous study, injection of sulfated polysaccharides shortly after pupation resulted in size modification of the B, DII, DI, and EII-EI elements (Serfas and Carroll 2005). Specifically, injections of heparin and heparan sulfate resulted in expansion of these patterns, whereas fucoidan and dextran sulfate resulted in contraction. Heparin and heparan

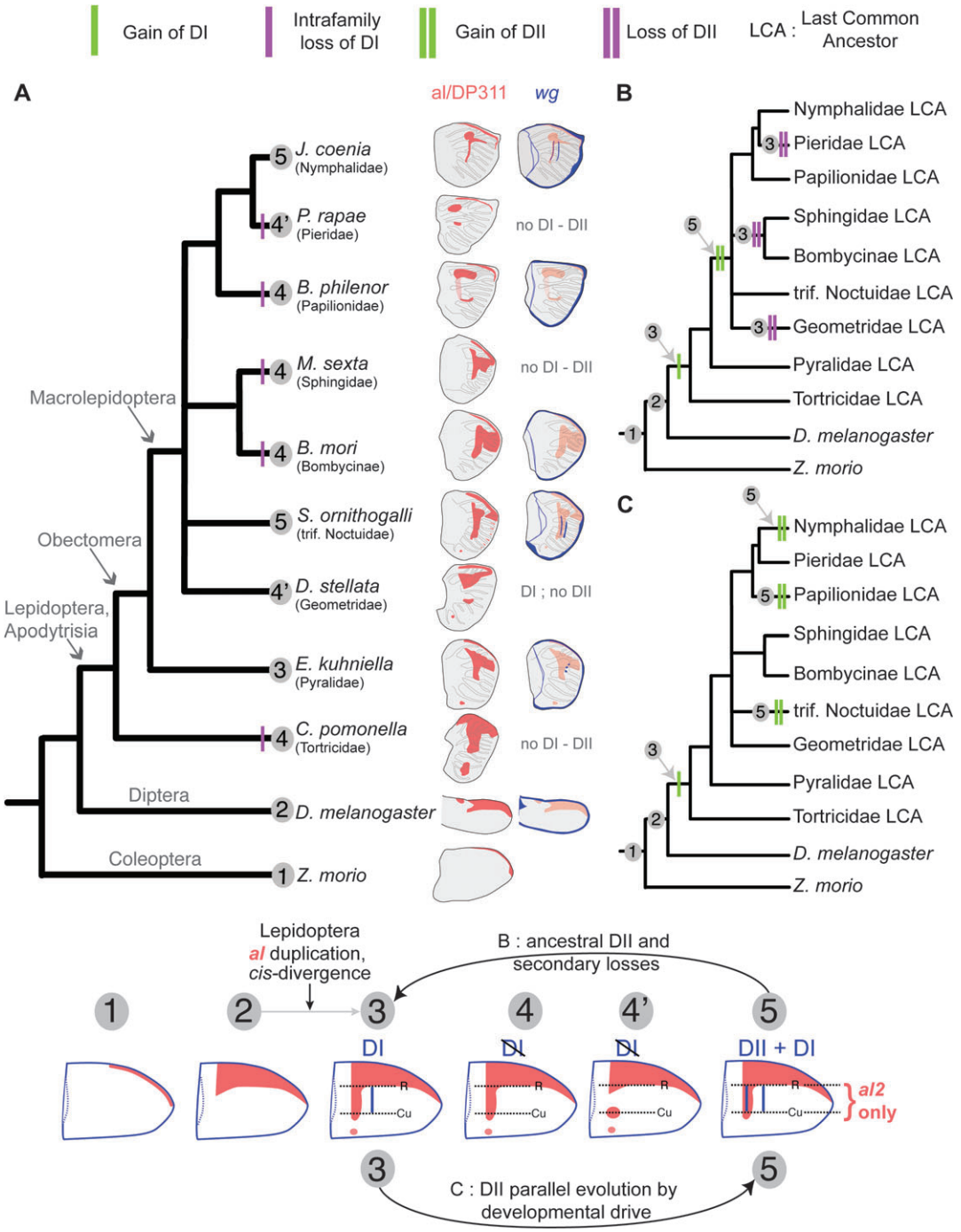

Fig. 6. Model for the evolution of DI and DII pattern elements. (*A*) Summary of forewing *wg* and DP311-antigen/*al* expression in the species sampled in this study. *Drosophila al* and *wg* expression are adapted from Campbell et al. (1993). Single purple bars signify that the absence of DI in the considered species may reflect a recent loss and an ancestral DI condition at the family level. (*B*–*C*) Developmental model for the evolution of forewing DII in Macrolepidoptera under the homology (*B*) and homoplasy (*C*) scenarios. 1: Putative holometabolous ancestral expression, with peripheral *wg* and costal *al*. 2: Putative mecopteridan ancestral expression, with extension of *al* in the anterior compartment. 3: Lepidopteran developmental ground plan, with continuous extension of *al2* in the posterior compartment and appearance of DI *wg* expression. *al1*/*al2* anterior expression is particularly strong in the penultimate instar but persists at low levels in the last-instar. 4–4′: Secondary, intrafamily (recent) loss of DI (and eventually DII) associated to the corresponding loss of *wg* expression. 4′: Denotes cases of discontinuous *al2* expression. 5: Complete DII + DI developmental ground plan, with *wg* recruited on a continuous stripe of *al2* expression between the radial (R) and cubital (Cu) tracheal trunks.

sulfate are structurally similar to the carbohydrate moiety of heparan sulfate proteoglycans (HSPGs)—extracellular matrix components known to enhance the activity of several signaling molecules (Lin 2004). This lead to the prediction that the symmetry axes of the B, DII, DI, and EI elements act as sources of a single morphogen that is deployed during early pupal stages to determine pattern width and color boundaries. In the present study, we found

that these predicted sources all express *wg*. Interestingly, it was previously shown in *Drosophila* that exogenous heparin and heparan sulfate increases extracellular solubility, stability, and distribution range of the wg ligand (Bradley and Brown 1990; Reichsman et al. 1996; Greco et al. 2001; Fuerer et al. 2010), and there is also genetic evidence that HSPGs and enzymes responsible for they sugar chain polymerization and sulfation are of prime importance for wg signaling (Binari et al. 1997; Blair 2005; Hacker et al. 2005; Gallet et al. 2008; Yan et al. 2009). Although this correlation does not rule out the possibility of additional heparin-sensitive signaling molecules such as other Wnt ligands or ligands of other signaling pathways, the *wg* expression pattern is sufficient to explain the effects of heparin injections by way of enhanced wg signaling. Under this model, the source cells of wg ligand are positioned at B, DII, DI, and EI before metamorphosis, and actual signaling occurs shortly after metamorphosis by extracellular transport of wg, which in turn acts to determine the width and color boundaries of the B, DII, DI, and EII-EI elements. Conversely, dextran sulfate and fucoidans likely act as competitive inhibitors of endogenous HSPGs and result in decreased wg signaling and smaller patterns. wg has also been reported in eyespot foci during early pupal stages (Monteiro et al. 2006). wg thus appears to be a central organizing molecule in wing patterning, offering an interesting case of parallelism with *Drosophila guttifera* wings (Werner et al. 2010). This model is also consistent with the numerous roles of the wg pathway in epithelial patterning (Barker 2008; Gonsalves and DasGupta 2008).

al2 expression in wing pattern development appears to be more complex than *wg*. This makes drawing correlations with color pattern somewhat more difficult. There are several consistent associations that are evident, however. First of all, DP311/*al2* is unambiguously expressed in a narrow stripe that corresponds exactly to the position of the DII *wg* expression in nymphalids, as evidenced by codetection assays (fig. 2 and supplementary fig. S3, Supplementary Material online). Temporally, DP311/*al2* always preceded *wg* DII expression across all lineages. Indeed, the DP311/*al2* stripe-pattern antigenicity in Nymphalidae and Noctuidae was readily observed at a very early stage, before tracheal introgression into the border lacunae, whereas DII-associated *wg* expression occurred only after tracheal ingression. This temporal succession of *al2* and *wg* expressions was especially evident in moths (Noctuidae and Pyralidae), where DP311/*al2* expression was obtained for 2–3 days before any *wg* central expression was detected in wing disks (stages corresponding to the left panels of supplementary fig. S2G and J, Supplementary Material online). The spatial and temporal associations between *wg* and *al2* in lepidoptera are consistent with the functional relationship of *al* and *wg* in *Drosophila* wing development, where ectopic *al* expression induces wing duplications associated with *wg* overexpression. Our findings suggest such a functional relationship might be conserved between lepidopteran *al2* and *wg* (Campbell et al. 1993). It will be interesting to test whether the al2 transcription factor directly or indirectly activates *wg* transcription in Lepidoptera.

In summary, our data lead us to speculate that sources of *wg* morphogen pattern some of the nymphalid ground plan elements, including B, DII, DI, and EI. Furthermore, the precise recruitment of *wg* expression in DP311-positive cells suggests a regulatory link between *al2* and *wg* (see in particular fig. 5*I*–*I*′). Finally, the conjecture that *al2* plays an functional role in patterning the DII element is supported by the correlation of *al2* expression with *L. arthemis* hindwing DII element, where a highly specific dislocation of the DII pattern is observed in *al2* expression as well (supplementary fig. S2*A*, Supplementary Material online).

Homology and Secondary Losses of DI Patterns in Lepidoptera

Forewing DI elements are present in most of the major families of Lepidoptera and appear to be a broadly conserved feature of the lepidopteran wing pattern ground plan (figs. 1 and 2). Also, as we have shown here, DI development is associated with *wg* expression in Nymphalidae, Noctuidae, and Pyralidae (fig. 4). This congruence of phylogenetic continuity and developmental similarity leads us to conclude that DI elements are homologous, at least throughout the Obectomera clade.

The peripheral expression of *wg* is conserved in Diptera (Campbell et al. 1993), Coleoptera (Tomoyasu et al. 2009), and Hymenoptera (Abouheif and Wray 2002), whereas central field *wg* expression in DI or other ground plan elements appears to have originated within the Lepidoptera lineage (fig. 6). This novel deployment of *wg* is likely to have occurred before the Obectomera radiation, and it would be interesting to see if it is retained in basal lepidopteran clades where DI occurs, such as in Hepialidae (e.g., *Z. stacyi*).

We found that, overall, DI was less frequent in hindwings than in forewings, both within and between families. This was not only true for moths, where hindwings are often hidden by the forewings and devoid of patterns, but also in butterflies, where hindwings are usually visible. We propose that hindwing DI elements be considered as serial homologs of their forewing counterparts. In fact, the observed phylogenetic discontinuity of DI distribution does not favor homoplasy between clades; rather, DI elements may be homologous and have undergone numerous losses in hindwings, for instance mediated by Ubx repression (Lewis et al. 1999; Weatherbee et al. 1999).

The Forewing DII Element: Labile Ancestral Trait or Homoplasy?

One could argue that *wg* expression in the presumptive forewing DII elements of both noctuids and nymphalids is an argument for their homology, that is, that their "positional" and "developmental" homologies are evidence for conservation in these lineages since the Nymphalidae–Noctuidae split (homology sensu stricto). But in contrast with the DI element that shows phylogenetic continuity throughout Lepidoptera, the forewing DII element shows a scattered distribution that suggests a complex history

of independent gains and losses (fig. 2, supplementary table S2, Supplementary Material online). Unfortunately, the deep, diverse, and partially unresolved phylogeny considered here makes it difficult to apply rigorous character state reconstruction methods in an informative way (Stone and French 2003).

When considering forewing DII evolution, there are two possible extreme scenarios, one based on extensive homology, the other based on extensive homoplasy (fig. 6). In the homology scenario, DII is ancestral and has undergone numerous secondary losses (for a more complete phylogeny, see fig. 2), which is consistent with the observed lability of DII elements at shallow levels, between species of the same genus (e.g., *Nymphalis*, *Heliconius*). In the homoplasy scenario, DII results from convergent evolution between the Nymphalidae, Papilionidae, and trifine Noctuidae lineages (fig. 6). This scenario is supported by examples of phylogenetically isolated DII elements, such as in Bombycoidea, where only one example of DII was encountered (*Hemileuca neumoegeni*, Saturniidae) and in Pyraloidea (Pyraustinae subfamily, Crambidae).

DII was never encountered outside of Obectomera, so we can conclude that it originated at least once in the Obectomera lineage. Based on the general supposition that trait loss is more likely than trait gain, and in the absence of a robust phylogenetic backbone, the DII homology scenario would be the most parsimonious hypothesis. This explanation would become less likely, however, if a simple biological mechanism could explain the repeated acquisition of the DII pattern element (see below).

Did *al2* Facilitate the Origin of the DII Pattern Element?

Based on the observations from our study, we hypothesize that *al2* expression represents spatial prepatterning information that may have facilitated the recruitment of *wg* during the evolution of DII in different lineages. First, we found that DII never occurs in the absence of DI, with only one possible exception in Notodontidae (fig. 2, supplementary table S2, Supplementary Material online). Together with the fact that both elements are patterned by *wg* expression, this suggests that DII patterns may be serial homologs of DI. In other words, DII patterning may be the result of the recruitment of the DI developmental module in the DII field, possibly by co-opting a new domain of *wg* expression. This hypothesis is consistent with the fact that DII and DI elements always have the same color composition in all the species we surveyed.

Second, we found that *al2* expression reports the existence of positional information in the DII field prior to the recruitment of *wg* DII expression. At a phylogenetic level, existence of this positional information in forewings is ancient and likely predated acquisition of the forewing DII color pattern element, as shown by DP311/*al2* continuous stripe expression in basal clades such as Tortricidae and Pyralidae. This is consistent with what is observed in hindwings, where the acquisition of a continuous *al2* stripe expression in Nymphalidae may have predated the only event of DII appearance among Lepidoptera hindwings. At least ancestrally, *al2* wing expression may have had functions other than DII patterning, which would be consistent with the fact that *al2* is not exclusively associated with *wg* and/or DII. For instance, the persistent radial and cubital tracheal trunk expression of DP311/*al2* produced, regardless of the wing or species, may indicate an ancestral role in wing vein development.

DP311/*al2* stripe expression may demonstrate the preexistence of positional information in the DII field that may have been used for the direct or indirect recruitment of *wg* expression. This scenario, where preexisting expression of a homeobox transcription factor biases evolution of a novel morphological trait, would be reminiscent of parallel evolution in *Drosophila* pigmentation (Gompel et al. 2005; Jeong et al. 2006; Prud'homme et al. 2006; Williams et al. 2008) and extremely similar to an example from *D. guttifera*, where *wg* itself was the target of recruitment during color pattern evolution (Werner et al. 2010). Under this model, evolution of the DII element and *Drosophila* pigment patterns could represent compelling examples of developmental drive (Arthur 2001, 2002).

Supplementary Material

Supplementary figures S1–S4 and tables S1–S2 are available at *Molecular Biology and Evolution* online (http://www.mbe.oxfordjournals.org/).

Acknowledgments

This research was supported by U.S. National Science Foundation grant DEB 0715140. We are particularly grateful to Nipam Patel for sharing the DP311/312 antibodies and to Suzanne Saenko and Riccardo Papa for sharing preliminary data. We thank Sean Mullen, Ronald Rutowski, Fred Nijhout, Laura Grunert, Richard Merrill, and Evelyne Hougardy who kindly provided live specimens, and Lawrence Gilbert for sharing insights on *H. cydno* genetics. We also thank Emily Daniels for help with rearing *J. coenia*, Michael Perry for technical advice, and Sophie Pantalacci and Francois Bonneton for their helpful comments on the manuscript.

References

Abouheif E, Wray GA. 2002. Evolution of the gene network underlying wing polyphenism in ants. *Science* 297:249–252.

Arthur W. 2001. Developmental drive: an important determinant of the direction of phenotypic evolution. *Evol Dev.* 3:271–278.

Arthur W. 2002. The interaction between developmental bias and natural selection: from centipede segments to a general hypothesis. *Heredity* 89:239–246.

Barker N. 2008. The canonical Wnt/beta-catenin signalling pathway. *Methods Mol Biol.* 468:5–15.

Beldade P, Brakefield PM. 2002. The genetics and evo-devo of butterfly wing patterns. *Nat Rev Genet.* 3:442–452.

Beldade P, Koops K, Brakefield PM. 2002. Modularity, individuality, and evo-devo in butterfly wings. *Proc Natl Acad Sci U S A.* 99:14262–14267.

Binari RC, Staveley BE, Johnson WA, Godavarti R, Sasisekharan R, Manoukian AS. 1997. Genetic evidence that heparin-like glycosaminoglycans are involved in wingless signaling. *Development* 124:2623–2632.

Bisby FA, Roskov YR, Orrell TM, Nicolson D, Paglinawan LE, Bailly N, Kirk PM, Bourgoin T, Baillargeon G. 2009. Species 2000 & ITIS Catalogue of Life: 2009 Annual Checklist. CD-ROM. In: 9th edn. (Species 2000), 2009.

Blair SS. 2005. Cell signaling: wingless and glypicans together again. *Curr Biol.* 15:R92–R94.

Bradley RS, Brown AMC. 1990. The protooncogene int-1 encodes a secreted protein associated with the extracellular-matrix. *EMBO J.* 9:1569–1575.

Brower AVZ, DeSalle R. 1998. Patterns of mitochondrial versus nuclear DNA sequence divergence among nymphalid butterflies: the utility of wingless as a source of characters for phylogenetic inference. *Insect Mol Biol.* 7:73–82.

Brunetti CR, Selegue JE, Monteiro A, French V, Brakefield PM, Carroll SB. 2001. The generation and diversification of butterfly eyespot color patterns. *Curr Biol.* 11:1578–1585.

Campbell G, Tomlinson A. 1998. The roles of the homeobox genes aristaless and Distal-less in patterning the legs and wings of Drosophila. *Development* 125:4483–4493.

Campbell G, Weaver T, Tomlinson A. 1993. Axis specification in the developing Drosophila appendage—the role of wingless, decapentaplegic, and the homeobox gene aristaless. *Cell* 74: 1113–1123.

Carroll SB, Gates J, Keys DN, Paddock SW, Panganiban GE, Selegue JE, Williams JA. 1994. Pattern-formation and eyespot determination in butterfly wings. *Science* 265:109–114.

Carroll SB, Grenier JK, Weatherbee SD. 2004. From DNA to diversity: Molecular genetics and the evolution of animal design, 2nd ed. Oxford: Blackwell Publishing.

Davis GK, D'Alessio JA, Patel NH. 2005. Pax3/7 genes reveal conservation and divergence in the arthropod segmentation hierarchy. *Dev Biol.* 285:169–184.

Edgar RC. 2004. MUSCLE: a multiple sequence alignment method with reduced time and space complexity. *BMC Bioinformatics.* 5:1–19.

Felsenstein J. 1989. PHYLIP—Phylogeny Inference Package (version 3.2). *Cladistics* 5:164–166.

Fuerer C, Habib SJ, Nusse R. 2010. A study on the interactions between heparan sulfate proteoglycans and Wnt proteins. *Dev Dyn.* 239:184–190.

Galant R, Skeath JB, Paddock S, Lewis DL, Carroll SB. 1998. Expression pattern of a butterfly achaete-scute homolog reveals the homology of butterfly wing scales and insect sensory bristles. *Curr Biol.* 8:807–813.

Gallet A, Staccini-Lavenant L, Therond PP. 2008. Cellular trafficking of the glypican Dally-like is required for full-strength Hedgehog signaling and wingless transcytosis. *Dev Cell.* 14:712–725.

Gilbert LE. 2003. Adaptive novelty through introgression in Heliconius wing patterns: evidence for shared genetic "tool box" from synthetic hybrid zones and a theory of diversification. In: Boggs CL, Watt WB, Ehrlich PR, editors. Butterflies: ecology and evolution taking flight. Chicago (IL): University of Chicago Press. p. 281–318.

Gompel N, Prud'homme B, Wittkopp PJ, Kassner VA, Carroll SB. 2005. Chance caught on the wing: cis-regulatory evolution and the origin of pigment patterns in Drosophila. *Nature* 433:481–487.

Gonsalves FC, DasGupta R. 2008. Function of the wingless signaling pathway in Drosophila. *Methods Mol Biol.* 469:115–125.

Greco V, Hannus M, Eaton S. 2001. Argosomes: a potential vehicle for the spread of morphogens through epithelia. *Cell* 106:633–645.

Hacker U, Nybakken K, Perrimon N. 2005. Heparan sulphate proteoglycans: the sweet side of development. *Nat Rev Mol Cell Biol.* 6:530–541.

Henke K, Krüse G. 1941. Uber Feldgliederungsmuster bei Geometriden und Noctuiden und den Musterbauplan der Schmetterlinge im Allgemein. Nachr Akad Wiss Gottingen, Math Physik Klasse. 1–48.

Jeong S, Rokas A, Carroll SB. 2006. Regulation of body pigmentation by the abdominal-B Hox protein and its gain and loss in Drosophila evolution. *Cell* 125:1387–1399.

Keys DN, Lewis DL, Selegue JE, Pearson BJ, Goodrich LV, Johnson RL, Gates J, Scott MP, Carroll SB. 1999. Recruitment of a hedgehog regulatory circuit in butterfly eyespot evolution. *Science* 283: 532–534.

Kristensen NP, Scoble MJ, Karsholt O. 2007. Lepidoptera phylogeny and systematics: the state of inventorying moth and butterfly diversity. *Zootaxa* 1668:699–747.

Kronforst MR, Kapan DD, Gilbert LE. 2006. Parallel genetic architecture of parallel adaptive radiations in mimetic Heliconius butterflies. *Genetics* 174:535–539.

Lafontaine JD, Fibiger M. 2006. Revised higher classification of the Noctuoidea (Lepidoptera). *Can Entomol.* 138:610–635.

Lewis DL, DeCamillis MA, Brunetti CR, Halder G, Kassner VA, Selegue JE, Higgs S, Carroll SB. 1999. Ectopic gene expression and homeotic transformations in arthropods using recombinant Sindbis viruses. *Curr Biol.* 9:1279–1287.

Lin XH. 2004. Functions of heparan sulfate proteoglycans in cell signaling during development. *Development* 131:6009–6021.

McDonald WP, Martin A, Reed RD. 2010. Butterfly wings shaped by a molecular cookie cutter: evolutionary radiation of lepidopteran wing shapes associated with a derived Cut/wingless wing margin boundary system. *Evol Dev.* 12:296–304.

Mitchell A, Mitter C, Regier JC. 2006. Systematics and evolution of the cutworm moths (Lepidoptera: Noctuidae): evidence from two protein-coding nuclear genes. *Syst Entomol.* 31:21–46.

Monteiro A, Glaser G, Stockslager S, Glansdorp N, Ramos D. 2006. Comparative insights into questions of lepidopteran wing pattern homology. *BMC Dev Biol.* 6:52–65.

Naisbit RE, Jiggins CD, Mallet J. 2003. Mimicry: developmental genes that contribute to speciation. *Evol Dev.* 5:269–280.

Nijhout HF. 1990. A comprehensive model for color pattern-formation in butterflies. *Proc R Soc Lond B Biol Sci.* 239:81–113.

Nijhout HF. 1991. The development and evolution of butterfly wing patterns. Washington (DC): Smithsonian Institution Press.

Nijhout HF. 1994. Symmetry systems and compartments in lepidopteran wings—the evolution of a patterning mechanism. *Development.* (Suppl):225–233.

Nijhout HF. 2001. Elements of butterfly wing patterns. *J Exp Zool.* 291:213–225.

Nijhout HF, Smith WA, Schachar I, Subramanian S, Tobler A, Grunert LW. 2007. The control of growth and differentiation of the wing imaginal disks of Manduca sexta. *Dev Biol.* 302:569–576.

Nijhout HF, Wray GA. 1988. Homologies in the color patterns of the genus Heliconius (Lepidoptera, Nymphalidae). *Biol J Linn Soc Lond.* 33:345–365.

Pohl N, Sison-Mangus MP, Yee EN, Liswi SW, Briscoe AD. 2009. Impact of duplicate gene copies on phylogenetic analysis and divergence time estimates in butterflies. *BMC Evol Biol.* 9:99.

Prud'homme B, Gompel N, Rokas A, Kassner VA, Williams TM, Yeh SD, True JR, Carroll SB. 2006. Repeated morphological evolution through cis-regulatory changes in a pleiotropic gene. *Nature* 440:1050–1053.

Quennedey A, Quennedey B. 1999. Development of the wing discs of Zophobas atratus under natural and experimental conditions: occurrence of a gradual larval-pupal commitment in the epidermis of tenebrionid beetles. *Cell Tissue Res.* 296:619–634.

Reed RD, Chen PH, Nijhout HF. 2007. Cryptic variation in butterfly eyespot development: the importance of sample size in gene expression studies. *Evol Dev.* 9:2–9.

Reed RD, Nagy LM. 2005. Evolutionary redeployment of a biosynthetic module: expression of eye pigment genes vermilion,

cinnabar, and white in butterfly wing development. *Evol Dev*. 7:301–311.
Reed RD, Serfas MS. 2004. Butterfly wing pattern evolution is associated with changes in a Notch/Distal-less temporal pattern formation process. *Curr Biol*. 14:1159–1166.
Regier JC, Cook CP, Mitter C, Hussey A. 2008. A phylogenetic study of the 'bombycoid complex' (Lepidoptera) using five protein-coding nuclear genes, with comments on the problem of macrolepidopteran phylogeny. *Syst Entomol*. 33:175–189.
Reichsman F, Smith L, Cumberledge S. 1996. Glycosaminoglycans can modulate extracellular localization of the wingless protein and promote signal transduction. *J Cell Biol*. 135:819–827.
Robinson-Rechavi M, Huchon D. 2000. RRTree: relative-rate tests between groups of sequences on a phylogenetic tree. *Bioinformatics* 16:296–297.
Ronquist F, Huelsenbeck JP. 2003. MrBayes 3: Bayesian phylogenetic inference under mixed models. *Bioinformatics*. 19:1572–1574.
Schlosser G, Wagner GP. 2004. Modularity in development and evolution. Chicago (IL): University of Chicago Press.
Schwanwitsch BN. 1924. On the ground-plan of wing pattern in Nymphalids and certain other families of Rhopalocerous Lepidoptera. *J Zool*. 34:509–528.
Schwanwitsch BN. 1943. Wing pattern in Papilionid Lepidoptera. *Entomologist, London*. 76:201–203.
Schwanwitsch BN. 1949. Evolution of the wing-pattern in the lycaenid Lepidoptera. *J Zool*. 119:189–263.
Schwanwitsch BN. 1956a. Color-pattern in Lepidoptera. *Ent Obozr, Moscow*. 35:530–546.
Schwanwitsch BN. 1956b. Wing pattern of pierid butterflies (Pieridae, Lepidoptera). *Ent Obozr, Moscow*. 35:285–301.
Seitz A. 1906. The Macrolepidoptera of the world; a systematic description of the hitherto known Macrolepidoptera. Stuttgart: Kernen Verlag.
Serfas MS, Carroll SB. 2005. Pharmacologic approaches to butterfly wing patterning: sulfated polysaccharides mimic or antagonize cold shock and alter the interpretation of gradients of positional information. *Dev Biol*. 287:416–424.
Smart P. 1991. The illustrated encyclopedia of the butterfly world. London: Tiger Books International.
Sokolov GN. 1936. Die Evolution der Zeichnung der Arctiidae. *Zool Jb (Anat)*. 61:107–238.
Stone G, French V. 2003. Evolution: have wings come, gone and come again? *Curr Biol*. 13:R436–R438.
Süffert F. 1927. Zur vergleichenden Analyse der Schmetterlingszeichnung. *Z Morph Oekol Tiere*. 47:385–413.
Suyama M, Torrents D, Bork P. 2006. PAL2NAL: robust conversion of protein sequence alignments into the corresponding codon alignments. *Nucleic Acids Res*. 34:W609–W612.
Tomoyasu Y, Arakane Y, Kramer KJ, Denell RE. 2009. Repeated co-options of exoskeleton formation during wing-to-elytron evolution in beetles. *Curr Biol*. 19:2057–2065.
Wahlberg N, Braby MF, Brower AVZ, et al. (11 co-authors). 2005. Synergistic effects of combining morphological and molecular data in resolving the phylogeny of butterflies and skippers. *Proc Biol Sci*. 272:1577–1586.
Weatherbee SD, Nijhout HF, Grunert LW, Halder G, Galant R, Selegue J, Carroll S. 1999. Ultrabithorax function in butterfly wings and the evolution of insect wing patterns. *Curr Biol*. 9:109–115.
Werner T, Koshikawa S, Williams TM, Carroll SB. 2010. Generation of a novel wing colour pattern by the Wingless morphogen. *Nature* 464:1143–1148.
Williams TM, Selegue JE, Werner T, Gompel N, Kopp A, Carroll SB. 2008. The regulation and evolution of a genetic switch controlling sexually dimorphic traits in Drosophila. *Cell* 134:610–623.
Wittkopp PJ. 2006. Evolution of cis-regulatory sequence and function in Diptera. *Heredity* 97:139–147.
Yan D, Wu Y, Feng Y, Lin S-C, Lin X. 2009. The core protein of glypican Dally-like determines its biphasic activity in wingless morphogen signaling. *Dev Cell*. 17:470–481.